International Journal of Advanced Research in Electronics and Communication Engineering (IJARECE)
Volume 3, Issue 4, April 2014

Different Atmospheric Turblence Levels and Noise Effects on Signal Transmission Efficiency in Terrestrial Free Space Optical Communication Networks

Ahmed Nabih Zaki Rashed[1*], and Mohamed A. Metawe'e[2]
[1]Electronics and Electrical Communications Engineering Department
Faculty of Electronic Engineering, Menouf 32951, Menoufia University, EGYPT
[2]Faculty of Engineering, Delta University for Engineering and Technology, EGYPT

***Abstract*—This paper has presented a analytical model description of free space optical (FSO) communication networks transmission performance under different atmospheric turbulence levels and noise effects. Link margin, signal transmission, signal quality, received signal power, particle size distribution, optical depth, transmission data rate, signal time delay spread, signal noise and signal attenuation are deeply studied over wide range of the affecting parameters. As well as the signal time delay spread and signal to noise ratio are deeply studied with using on-off keying (OOK) modulation scheme and are compared with their simulation results by using binary phase shift keying modulation technique.**

***Index Terms*— Particle size distribution, Optical depth, Fog Density levels, Optical path length, Noise effects, and link margin.**

I. Introduction

Vertical cavity semiconductor emitting laser (VCSEL) Laser transmitting system consists of laser transmitter, laser driver and optical transmitting antenna. Comparing to the conventional semiconductor emitting laser (EEL), the VCSEL, as the laser transmitter, its circle thin beam has the advantages of smaller far field angle of divergence and easier to couple into optical fiber [1]. The average power, not the peak power, determines the link margin. Because of their high efficiency, power dissipation is typically not an issue for VCSELs, and active cooling is not required. In addition, VCSEL has the characteristics of low threshold current, high modulating frequency and operating of single longitudinal mode in broad range of temperature and current [2-3]. The avalanche photodiode (APD) is used as a receiver with a dark current of 1 μA. APD's are essentially p-i-n devices that are operated at very high reverse bias, so that photo generated carriers create secondary carriers by impact ionization, resulting in internal electrical gain. APD's are favored in direct detection optical receivers when there is little ambient-induced shot noise, because their internal gain helps overcome preamplifier thermal noise, increasing the receiver signal to noise ratio (SNR). APD based receivers can lead to impressive infrared link performance when ambient light is weak [4]. Atmospheric attenuators like fog, rain, snow, mist and haze severely degrade the system performance. Absorption and scattering of radiation from fog, clouds, dust, snow and smoke cause significant attenuation of a laser beam propagating through the atmosphere. Fog and clouds are typical dominating factors causing atmospheric attenuation over a considerable period of the time [5].

FSO is the concept of transmitting very high bandwidth digital data using laser beam directly through the atmosphere. Recently FSO links are identified as an attractive alternative to the existing radio links for applications involving ground-to-ground (short and long distance terrestrial links), satellite uplink/downlink, intersatellite, and satellite. Moreover, growing demands for higher data rates and wider bandwidths from the end user to manipulate multimedia information in the recent years allegorizes a challenge for the future next generation networks (NGN). The prime advantages of FSO usage are: a wider bandwidth with data rates exceeding easily 100 Gb/sec using wavelength division multiplexing (WDM) techniques, low power consumption, better security against eavesdropping, better protection against interference, and no frequency regulation issues [6-8]. However, a well known disadvantage of FSO links in the troposphere is their sensitivity to weather conditions primarily to fog and precipitation, causing substantial loss of the optical power over the channel path [9, 10]. Even though, if fog, snow and rain concerns only a small fraction of the time and or affects only a small portion of the overall propagation path yet it severely impairs the optical link performance and limits the communication link availability primarily due to the Mie scattering phenomena [11, 12].

II. Terrestrial Free Space Optical Communication Link

FSO communications gives user, large and unregulated bandwidth. The free space optical communication uses the light signal which carries the information. This light signal is not confined into a physical channel like optical fiber. In the free space optical communication the optical signal is transmitted into the free space and the air or vacuum space acts as the channel for signal transmission. The FSO can provide data rate in the range of 100 Gb/s and the data transfer is achievable over a distance of 1-4 km. The direct line-of-sight FSO link offer numerous advantages compared to the conventional wired and radio frequency (RF) wireless communications [13-15].

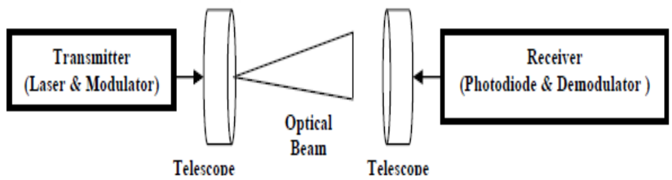

Fig. 1. Schematic view of free space optical link.

ISSN: 2278 – 909X

A block diagram of an FSO communication link is presented in Fig. 1. The transmitter modulates data onto the instantaneous intensity of an optical beam. Intensity modulated direct detection channels using on off keying (OOK) modulation, which is widely employed in practical systems. The received photocurrent signal is related to the incident optical power by the detector responsivity R. It is assumed that the receiver integrates the photocurrent for each bit period and removes any constant bias due to background illumination. The performance of the FSO link is hampered by some atmospheric conditions such as fog, rain, snow etc. There are few other circumstances when the performance of the FSO system may get affected which include building sway during earthquake or some temporary blockage between line of sight connections required for data transmission [16, 17].

III. System Modeling Analysis

Light propagating through fog is scattered on water droplets. As the droplet diameter is comparable to wavelength, the process is described by the Mie theory. The type of fog is characterized by particle size distribution (number of particles per unit volume (cm^{-3}) per unit increment of radius (μm)), which is usually approximated by the normalized modified particle size distribution as [18]:

$$n(r) = a\, r^{w} \exp(-b\, r) \quad (1)$$

Where r is the particle radius, and a, b, and w are coefficients according to the type of fog as in Ref. [18]. Radiation (continental) fog generally appears during the night and at the end of the day, particularly in valleys. Advection (maritime) fog is formed by the movement of wet and warm air masses above the colder maritime or terrestrial surfaces. Actual fog parameters may vary significantly for individual fog events [18]. The scattering coefficient can be expressed as a function of the visibility and wavelength. The scattering coefficient in hazy days can be determined by using the following formula [19]:

$$\beta = \frac{3.912}{V}\left(\frac{550\, nm}{\lambda}\right)^{q} \quad (2)$$

Where V is the visibility in meters, λ is the optical signal wavelength in nanometers and q is the size distribution of the scattering particles (q=V-0.5 for 500 m<V<1000 m, and q=0.01 for V<500 m). The atmospheric attenuation is described by the following Beer's Law equation [19]:

$$\alpha = 10 \log \exp(\beta L) \quad (3)$$

Where L is the optical path length. As well as the signal transmission, T_{fog} can be described by the following equation:

$$T_{fog} = \exp(-\beta\, L) \quad (4)$$

It is possible to identify a fog condition with a visibility range and relate it to the optical attenuation by using the Kruse formula. However, this formula is inapplicable to fog because the wavelength dependence of fog is too small in the visible and infrared range [20]. Fogs are composed of very fine water droplets of water, smoke, ice or combination of these suspended in the air near the Earth's surface [6]. The presences of these droplets act to scatter the light and so reduce the visibility near the ground. A fog layer is reported whenever the horizontal visibility at the surface is less than 1 km [6, 21]. Normally, after sunset a strong cooling takes place near the earth surface through the divergence effect of long wave radiation. Therefore it is necessary to specify a fog condition with a parameter that is more general than a visibility range. The parameter that indicates the thickness of fog is the optical depth. Optical depth generally indicates the average number of interactions that light will incur when propagating through a multiple-scatter channel. The optical depth τ is defined as a function of atmosphere attenuation and optical path length as follows [20]:

$$\tau = \frac{\alpha\, L}{4.34} \quad (5)$$

Consider a laser transmitting a total signal power P_S at the specified wavelength. The signal power received, P_R at the communications detector can be expressed as [21]:

$$P_R = P_S\, \frac{D_R}{\theta\, L^2} 10^{-\alpha L/10} \eta_T\, \eta_R \quad (6)$$

Where D_R is the receiver diameter, θ is the transmitter divergence angle, α is the atmospheric attenuation factor (dB/m), η_T, η_R are the transmitter and receiver optical efficiency respectively. As well as the achievable data rate R can be obtained from [21]:

$$R = \frac{P_S\, P_R\, 10^{-\alpha L/10} D_R^2}{\pi\left(\frac{\theta}{2}\right)^2 L^2\, E_P\, N_b} \quad (7)$$

Where E_P=hc/λ is the photon energy at wavelength λ and N_b is the receiver sensitivity. Another important parameter in optical communications link analysis is "Link Margin", which is the ratio of available received power to the receiver power required to achieve a specified bit error rate (BER) at a given data rate. Note that the required power at the receiver to achieve a given data rate, R (Tb/s), we can define the link margin LM as [21]:

$$LM = \left(\frac{P_S\, \lambda}{N_b\, R h c}\right)\left(\frac{D_R^2}{\theta^2\, L^2}\right) 10^{-\alpha L/10} \eta_T\, \eta_R \quad (8)$$

By using the least squares method, a simple quadratic relationship between the time delay spread, D and the optical depth, τ is expressed as the following formula [22]:

$$D = 9.9x10^{-11}\tau^2 - 1.4x10^{-9}\tau - 1.9x10^{-9} \quad (9)$$

Noise in the system depends on the characteristics of a receiver. A receiver is basically composed of photodetector and detection components. A photodetector changes the optical signal to an electrical signal. Detection components process and demodulate an electrical signal. A simple OOK system with an integrate and dump receiver, so that the transmitter and receiver filters are identical and its behavior is similar to a bandpass filter. The optical signal with OOK encoding carries no negative power, but when optical signal is converted to an electrical signal, both DC and AC components occur. The DC component is filtered out before the detection process and that only the AC component undergoes maximum-likelihood detection [20]. The background power noise can be defined by:

$$P_{BG} = H_{KBG}\, \pi (FOV)^2 A_R\, \Delta\lambda\, T_F \exp(\tau) \quad (10)$$

Where H_{KBG} is the background radiance, FOV is the receiver field of view, A_R is the receiver area defined as A_R= $\pi(D_R/2)^2$, Δλ is fiber optic bandwidth, and T_F is the filter transmissivity. For noise consideration, the variances in detected current resulting from background radiation, thermal and shot noise are defined as [20]:

ISSN: 2278 – 909X

$\sigma_{BG} = \sqrt{2q\zeta P_{BG} B}$, $\sigma_{TH} = \sqrt{(4kT_e F B)/R_L}$,

$$\sigma_{SS} = \sqrt{2q\zeta P_R B} \quad (11)$$

Where F is the noise figure, k is the Boatmen's constant, T_e is the equivalent temperature, q is the electron charge, B is the detector electronic bandwidth, and ζ is the responsivity (in amperes per watt) is used to characterize the efficiency of a photodiode in converting light to an electrical signal. However, interested in correlating the Q-factor for a range of transmittance of the received signal and for different fog conditions. The Q-factor, which represents the signal to noise ratio (SNR) at the receiver with no fog, is given as:

$$Q = T_0 \frac{I_1 - I_0}{\sigma_0 + \sigma_1} \quad (12)$$

Where T_0 is the maximum transmittance and is equal to the unity. I_1 and I_0 are the average detected signal current for bit '1' (on state) and '0' (off state) where as σ_0 and σ_1 are the standard deviation of the noise values for bit '1' and '0' which are defined by [23, 24]:

$$I_1 = \zeta (P_R + P_{BG}), \ \sigma_1 = \sqrt{\sigma_{SS}^2 + \sigma_{TH}^2 + \sigma_{BG}^2} \quad (13)$$

$$I_0 = \zeta P_{BG}, \ \sigma_0 = \sqrt{\sigma_{TH}^2 + \sigma_{BG}^2} \quad (14)$$

However, with fog and assuming the ambient noise level does not change with fog density, the Q-factor in dB Units can be approximated as [24]:

$$Q_{fog}(dB) = 10 \log_{10} T_{fog} Q \quad (15)$$

IV. Numerical Simulation and Performance Analysis

Optical signals transmitted through free-space are affected by temporal and spatial variations in the channel causing amplitude fades and frequency distortions. Therefore in the present study, we have investigated optical wireless communication systems operation performance efficiency evaluation in the presence of different fog density levels and noise impact over wide range of the affecting operating parameters as shown in Table 1.

Table 1: List of system parameters used in the simulation [5, 12, 19, 20, 21, 24].

Parameter	Definition	Value and unit
V_d (Dense fog)	Visibility range with dense fog	40 m-70 m
V_t (Thick fog)	Visibility range with thick fog	70 m-250 m
V_m (Moderate fog)	Visibility range with thick fog	250 m-500 m
V_l (Light fog)	Visibility range with light fog	500 m-1000 m
λ	Optical signal wavelength	850 nm-1550 nm
P_S	Transmitted optical power	100 mW
η_T	Transmitter efficiency	0.9
η_R	Receiver efficiency	0.9
D_R	Receiver diameter	10 cm
θ	Transmitter divergence angle	2 mrad
N_b	Receiver sensitivity	-30 dBm
c	The light velocity	$3x10^8$ m/sec
h	Plank's constant	$6.6x10^{-34}$ J/sec
L	Optical path length	100 m-1000 m
H_{KBG}	Background radiance	$0.2 Wm^{-2} nm^{-1} sr^{-1}$
FOV	Receiver field of view	5 mrad-50 mrad
Δλ	Filter optic bandwidth	10 nm
T_F	Filter transmissivity	0.5
q	Electron charge	$1.6x10^{-19}$ C
B	Detector electronic bandwidth	10 MHz
ζ	Receiver responsivity	0.9 A/W
F	Noise figure	2.5 dB
k	Boltzmann's constant	1.381×10^{-23} J/K
T_e	Equivalent temperature	300 K
r	Particle radius	1 μm-30 μm

Based on the model equations analysis, assumed set of the operating parameters, and the set of the series of the Figs. (2-27), the following facts are assured:

i) Fig 2 has assured that particle size distribution has maximum coverage area in the case of dense fog in compared with other fog density levels.

ii) Figs. (3-6) have indicated that as visibility with different fog density levels increases, this leads to decrease in signal scattering coefficient. As well as operating optical signal wavelength increases, this results in decreasing of signal scattering coefficient for different fog density levels under study consideration. It is theoretically observed that dense fog level has presented maximum signal scattering in compared with other fog density levels.

ISSN: 2278 – 909X

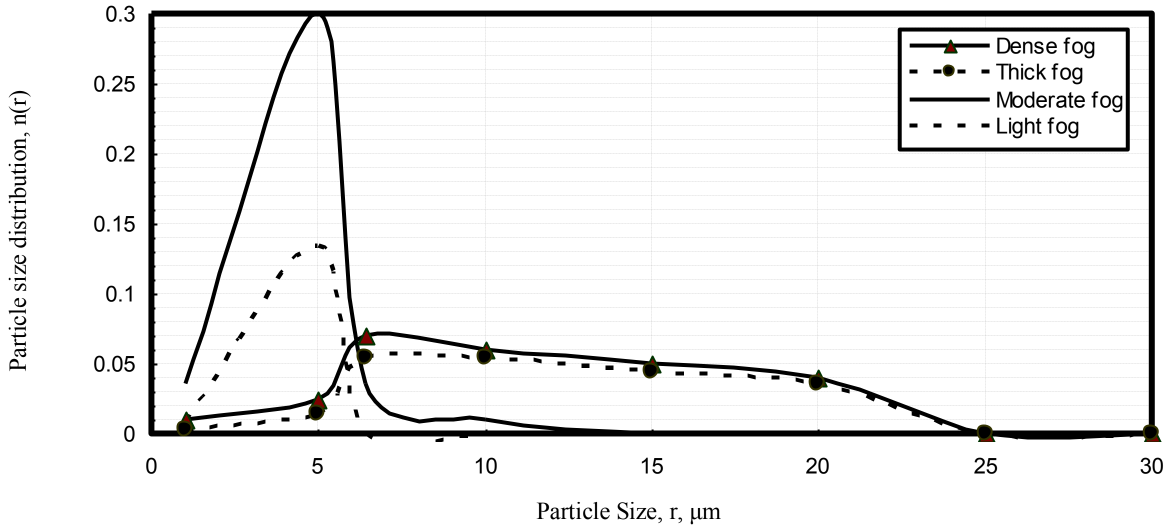

Fig. 2. Variations of particle size distribution versus particle size for different fog density levels at the assumed set of the operating parameters.

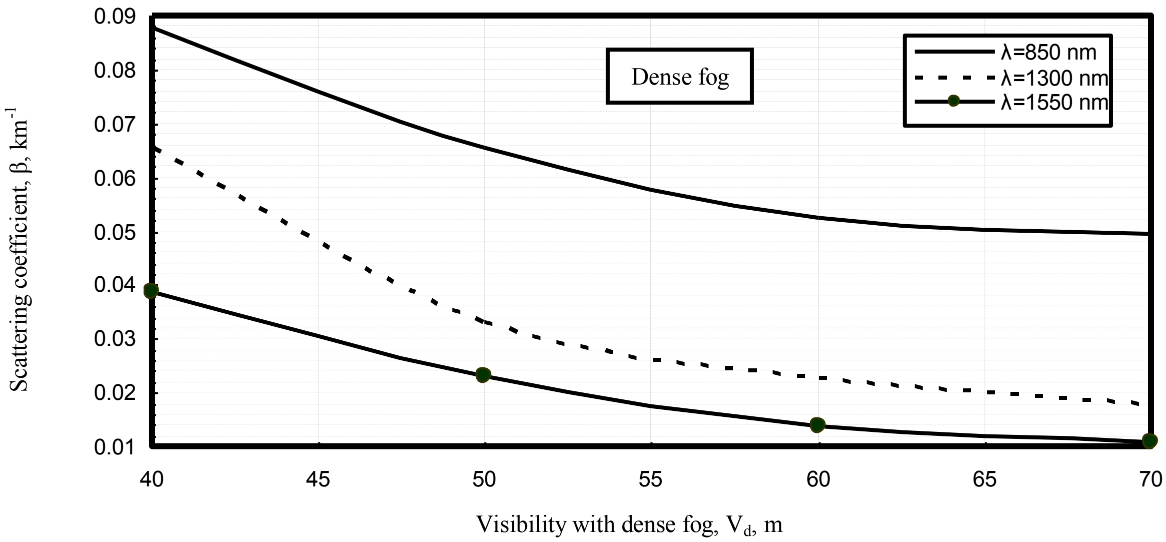

Fig. 3. Scattering coefficient in relation to visibility with dense fog and different operating optical signal wavelengths at the assumed set of the operating parameters.

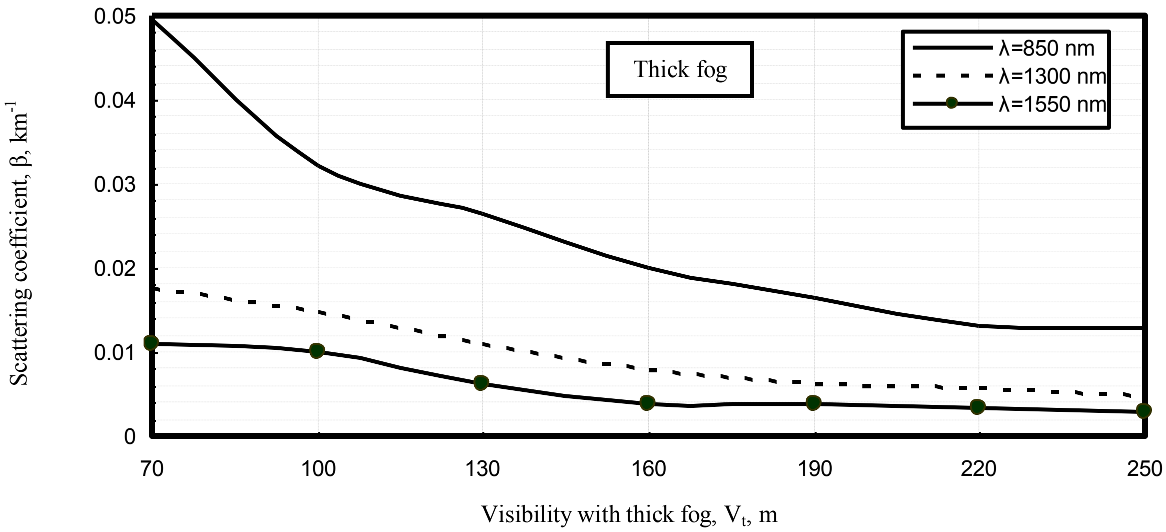

Fig. 4. Scattering coefficient in relation to visibility with thick fog and different operating optical signal wavelengths at the assumed set of the operating parameters.

ISSN: 2278 – 909X

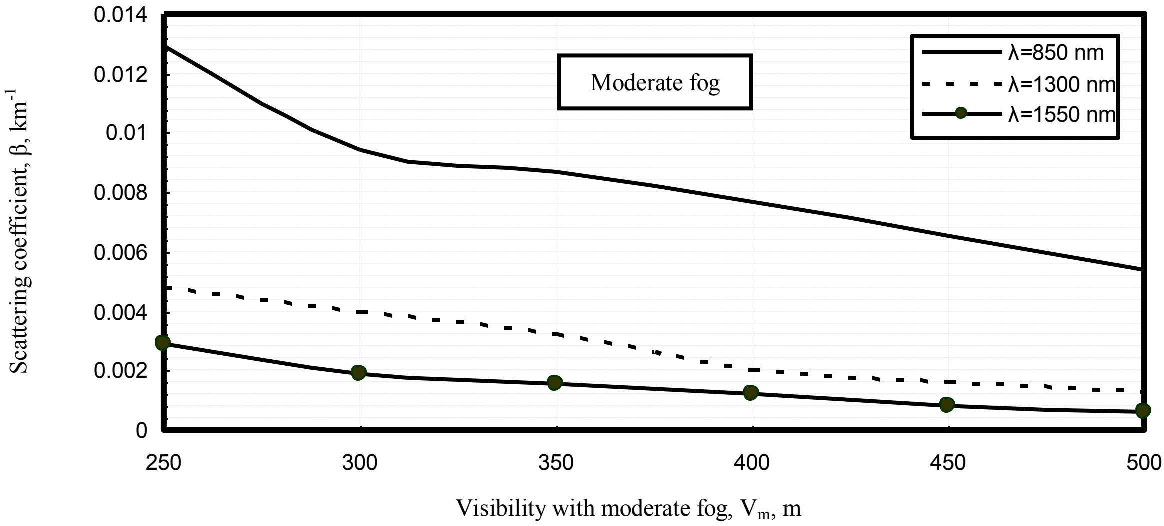

Fig. 5. Scattering coefficient in relation to visibility with moderate fog and different operating optical signal wavelengths at the assumed set of the operating parameters.

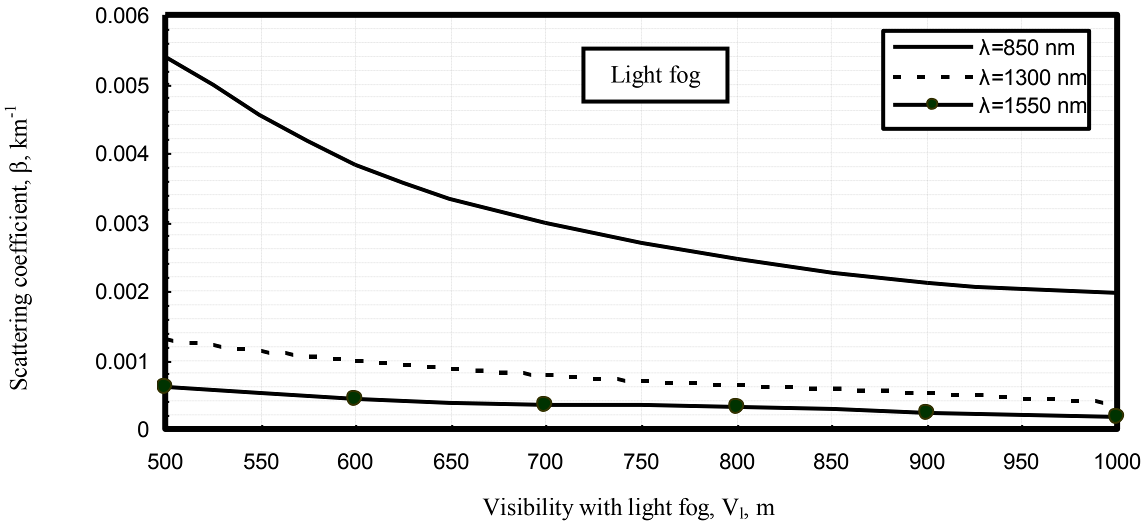

Fig. 6. Scattering coefficient in relation to visibility with light fog and different operating optical signal wavelengths at the assumed set of the operating parameters.

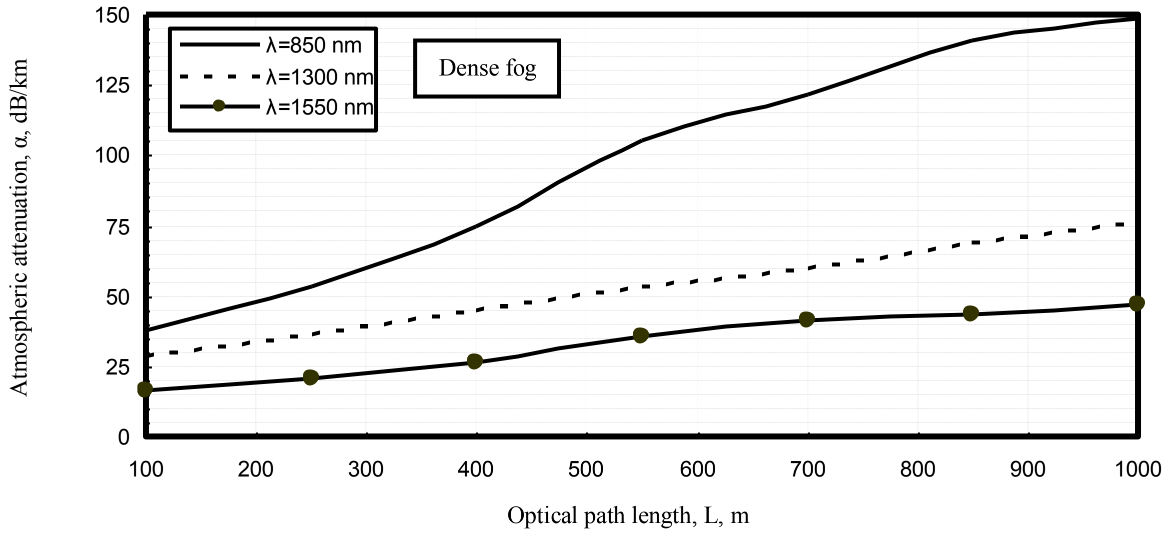

Fig. 7. Atmospheric signal attenuation in relation to optical path length with dense fog and different operating optical signal wavelengths at the assumed set of the operating parameters.

ISSN: 2278 – 909X

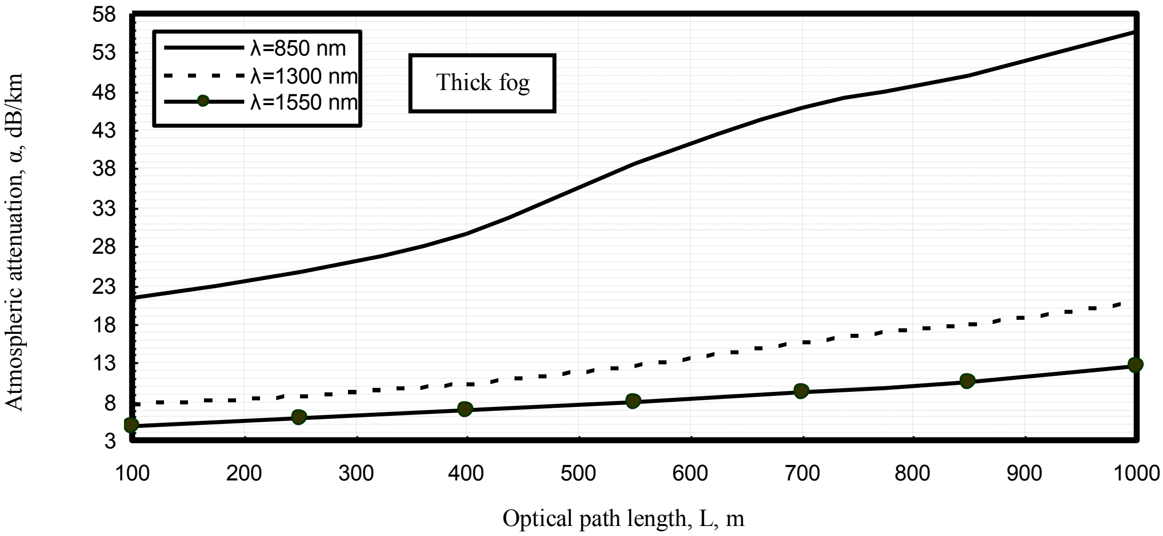

Fig. 8. Atmospheric signal attenuation in relation to optical path length with thick fog and different operating optical signal wavelengths at the assumed set of the operating parameters.

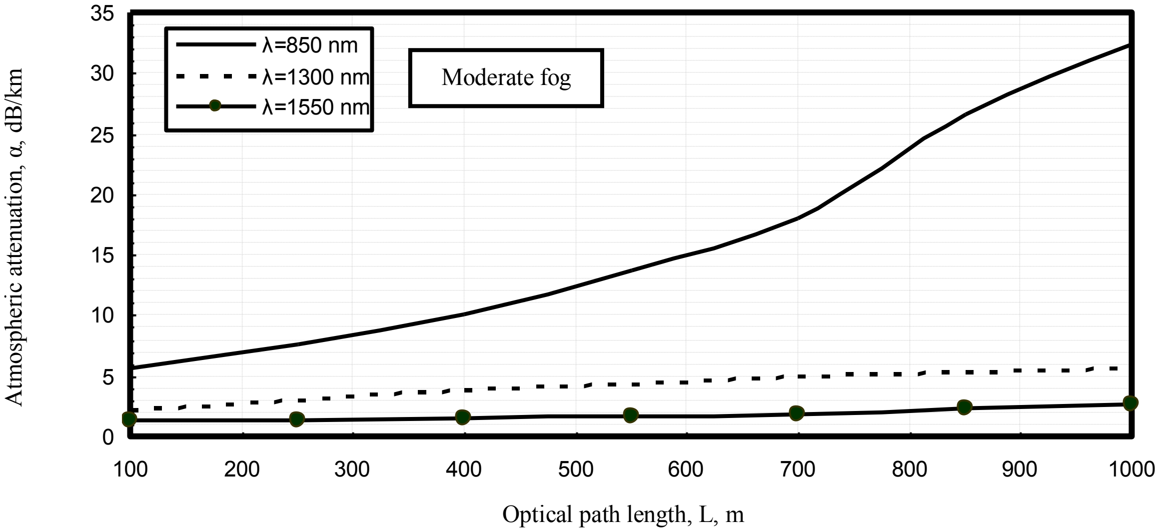

Fig. 9. Atmospheric signal attenuation in relation to optical path length with moderate fog and different operating optical signal wavelengths at the assumed set of the operating parameters.

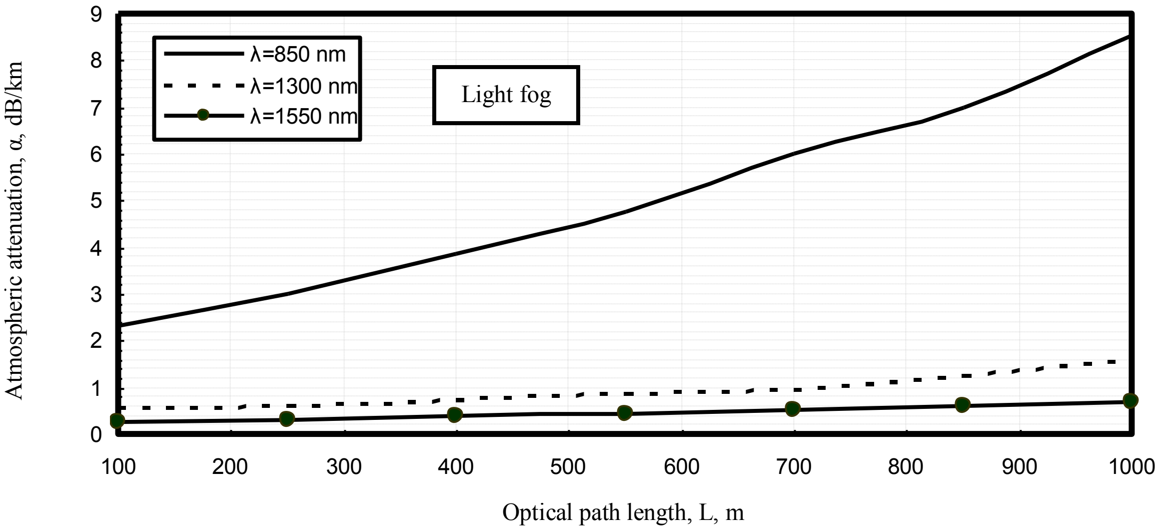

Fig. 10. Atmospheric signal attenuation in relation to optical path length with light fog and different operating optical signal wavelengths at the assumed set of the operating parameters.

ISSN: 2278 – 909X

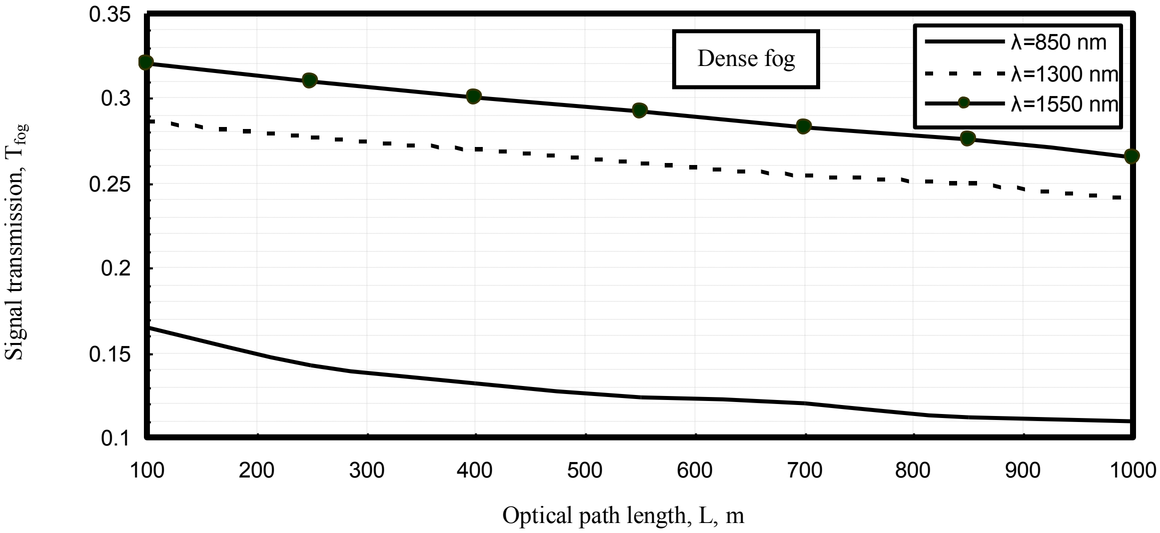

Fig. 11. Signal transmission in relation to optical path length with dense fog and different optical transmission windows at the assumed set of the operating parameters.

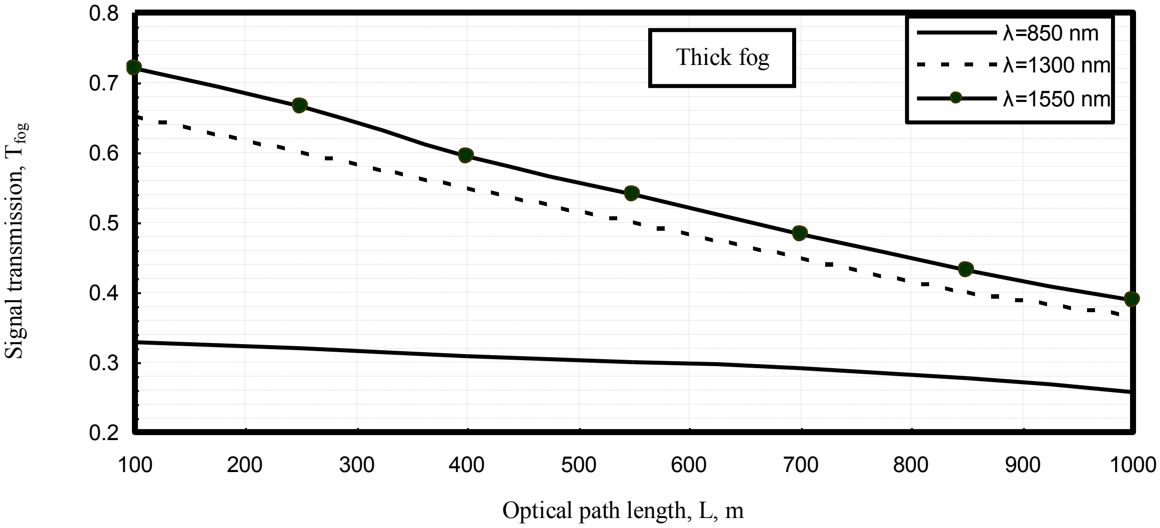

Fig. 12. Signal transmission in relation to optical path length with thick fog and different optical transmission windows at the assumed set of the operating parameters.

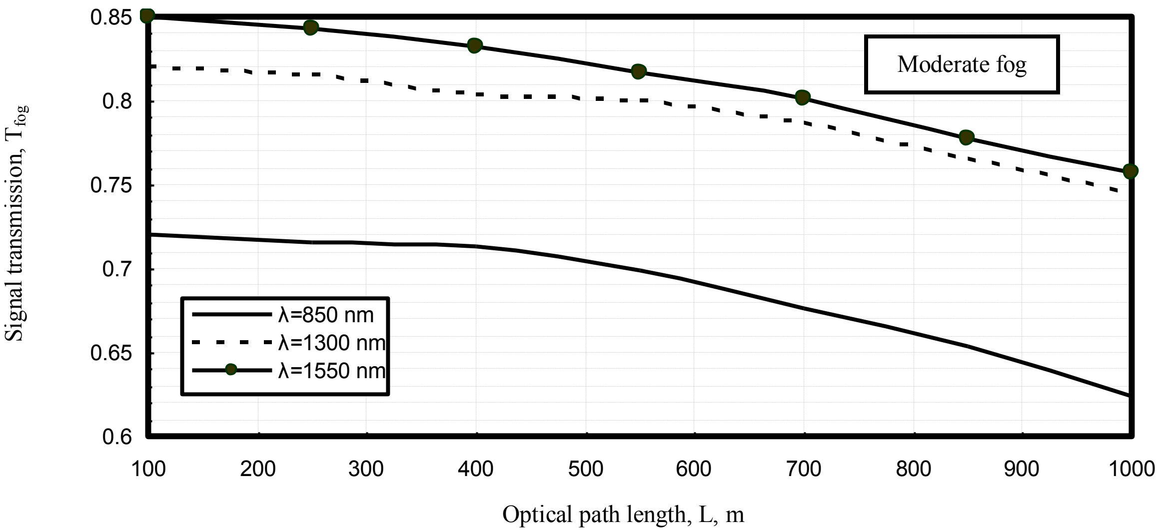

Fig. 13. Signal transmission in relation to optical path length with moderate fog and different optical transmission windows at the assumed set of the operating parameters.

ISSN: 2278 – 909X

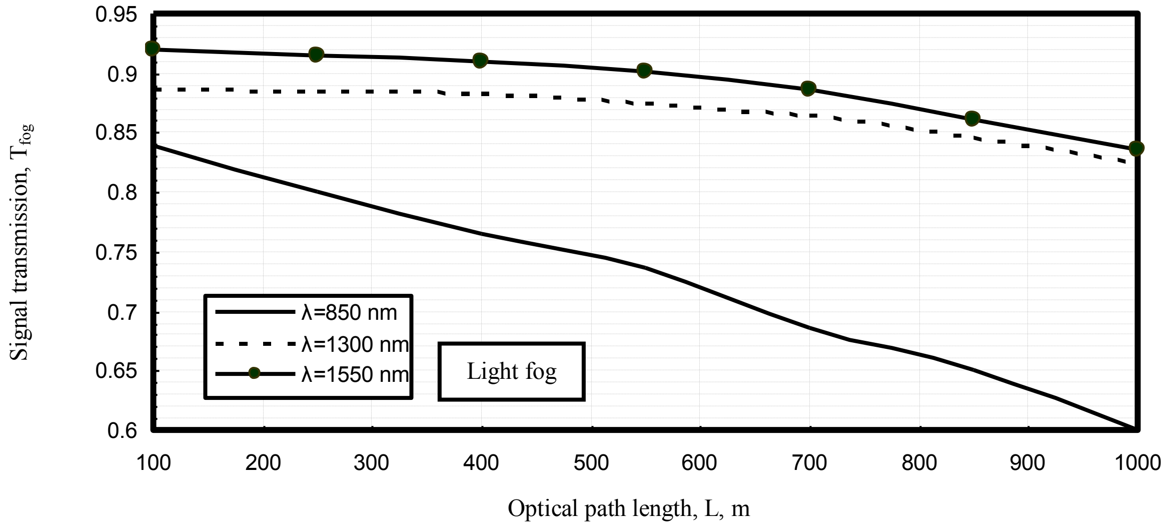

Fig. 14. Signal transmission in relation to optical path length with light fog and different optical transmission windows at the assumed set of the operating parameters.

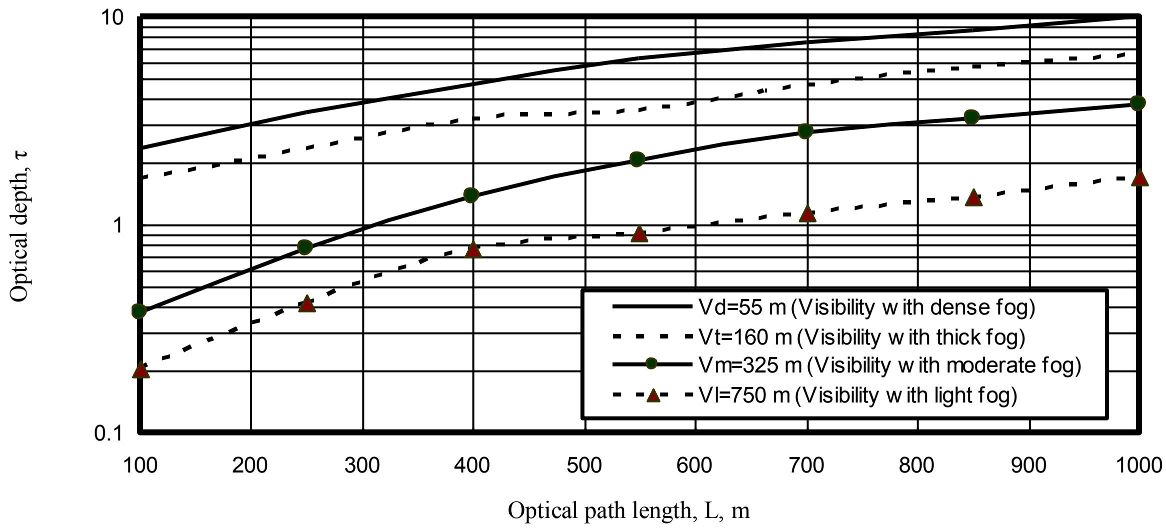

Fig. 15. Optical depth in relation to optical path length with visibilities at different fog density levels and operating optical signal wavelength λ=1550 nm at the assumed set of the operating parameters.

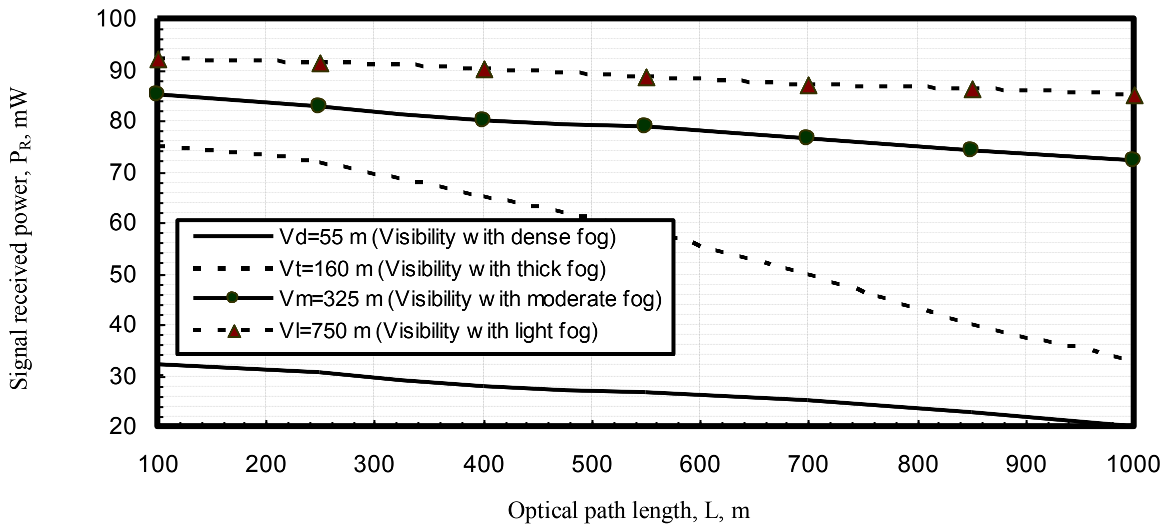

Fig. 16. Received signal power in relation to optical path length with visibilities at different fog density levels and operating optical signal wavelength λ=1550 nm at the assumed set of the operating parameters.

ISSN: 2278 – 909X

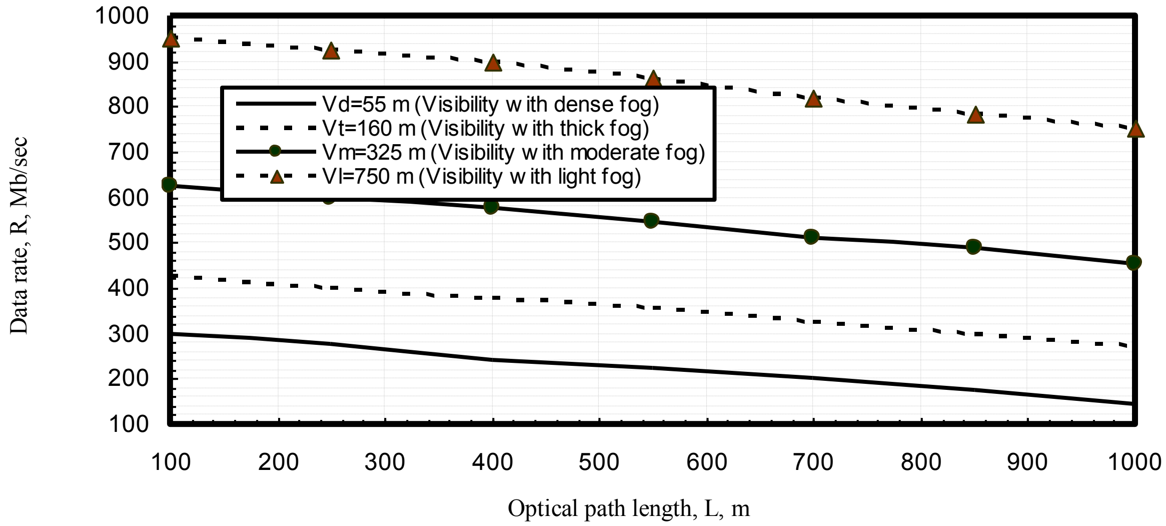

Fig. 17. Transmission data rate in relation to optical path length with visibilities at different fog density levels and operating optical signal wavelength λ=1550 nm at the assumed set of the operating parameters.

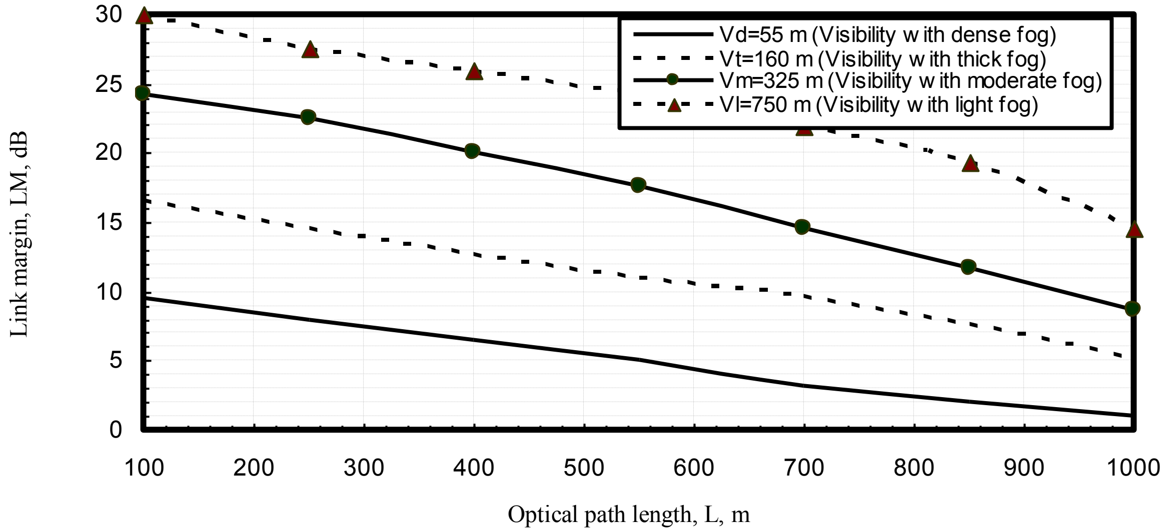

Fig. 18. Link margin in relation to optical path length with visibilities at different fog density levels and operating optical signal wavelength λ=1550 nm at the assumed set of the operating parameters.

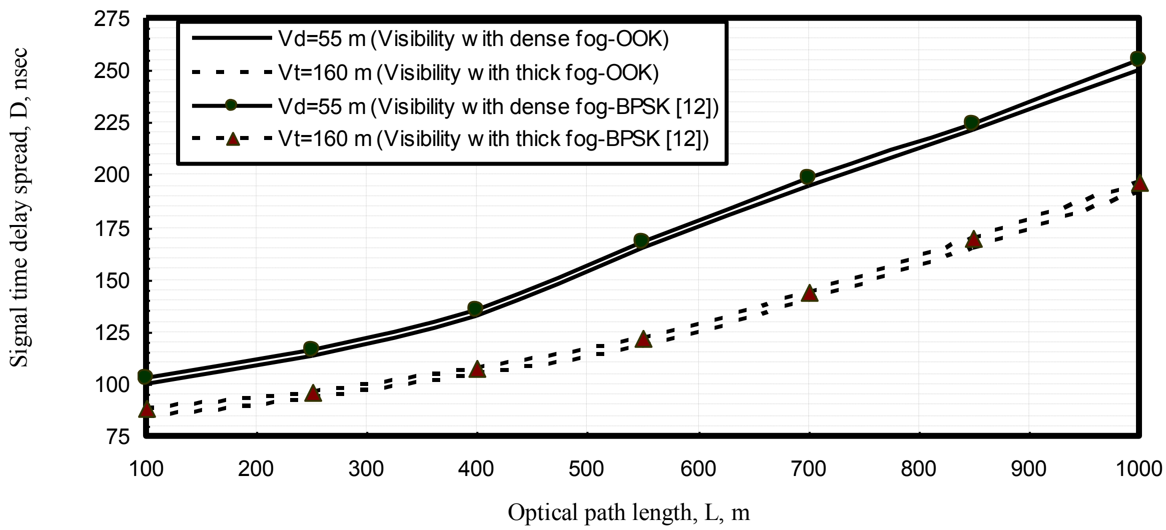

Fig. 19. Signal time delay spread in relation to optical path length with visibilities at different fog density levels (dense and thick fog) and operating optical signal wavelength λ=1550 nm at the assumed set of the operating parameters.

ISSN: 2278 – 909X

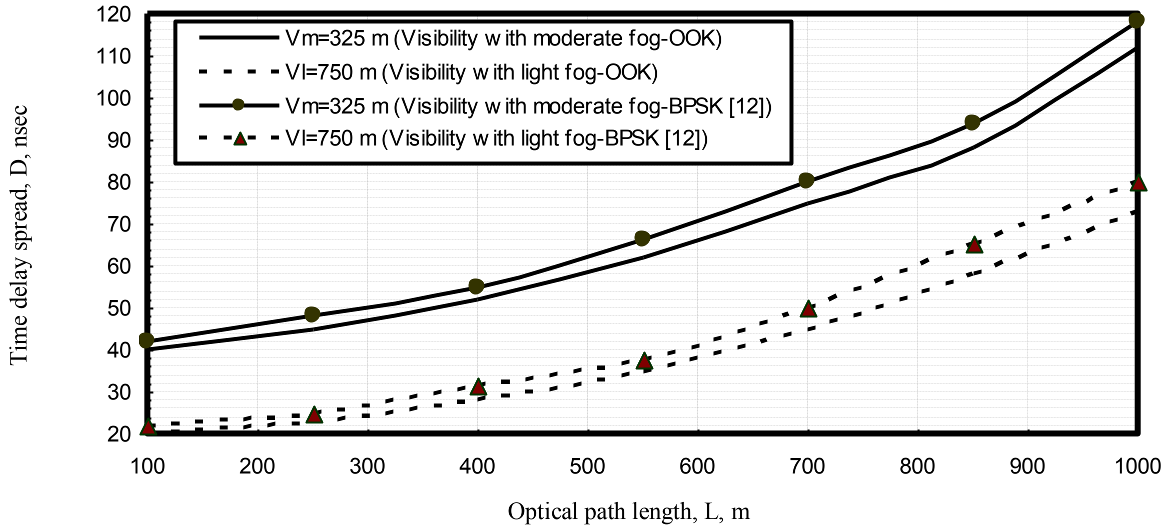

Fig. 20. Signal time delay spread in relation to optical path length with visibilities at different fog density levels (moderate and light fog) and operating optical signal wavelength λ=1550 nm at the assumed set of the operating parameters.

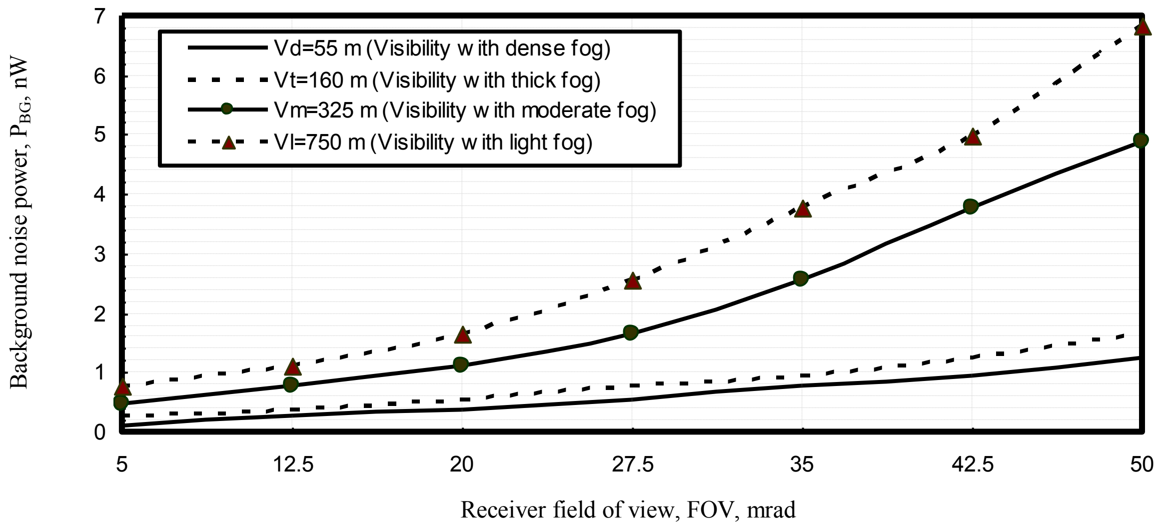

Fig. 21. Variations of background noise power versus variations of receiver field of view with visibilities at different fog density levels and optical path length L=100 m at the assumed set f the operating parameters.

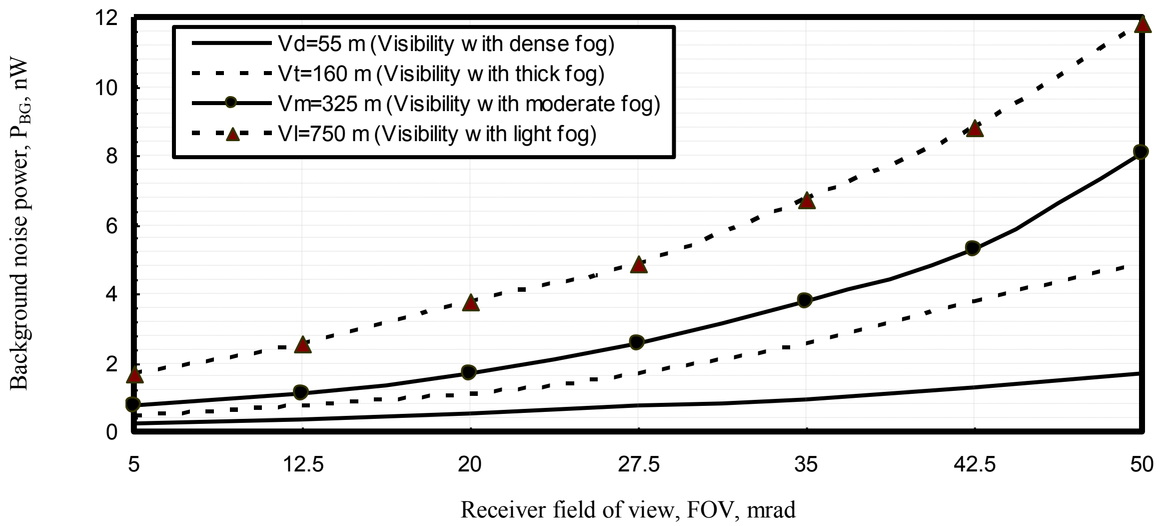

Fig. 22. Variations of background noise power versus variations of receiver field of view with visibilities at different fog density levels and optical path length L=500 m at the assumed set f the operating parameters.

ISSN: 2278 – 909X

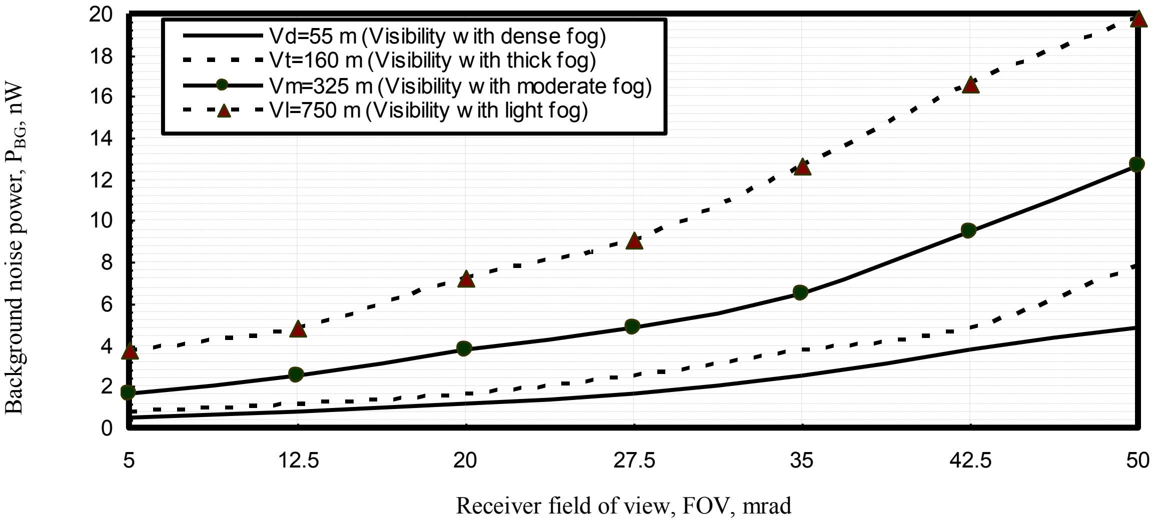

Fig. 23. Variations of background noise power versus variations of receiver field of view with visibilities at different fog density levels and optical path length L=1000 m at the assumed set f the operating parameters.

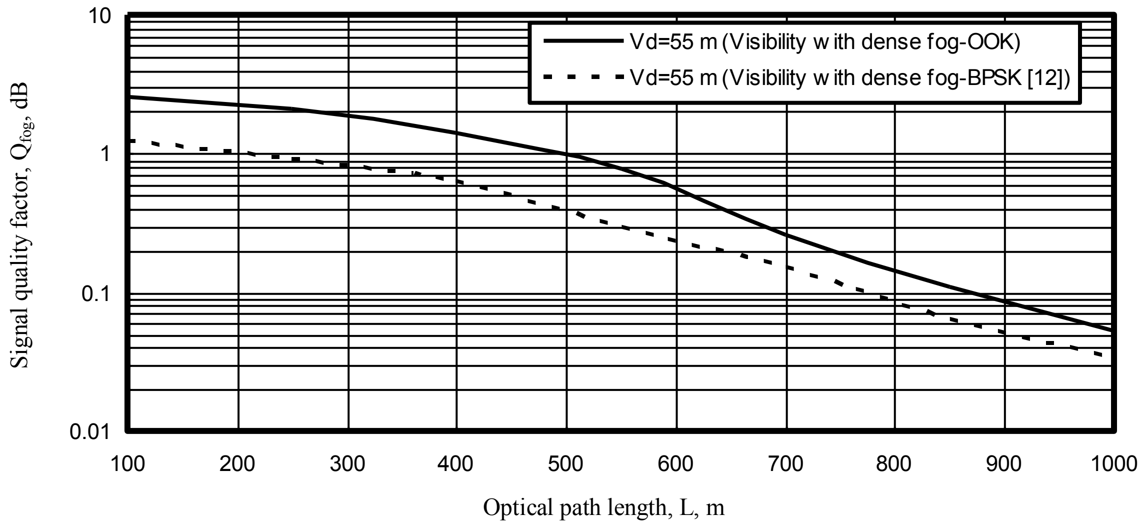

Fig. 24. Signal quality factor in relation to optical path length and visibility with dense fog at the assumed set of the operating parameters.

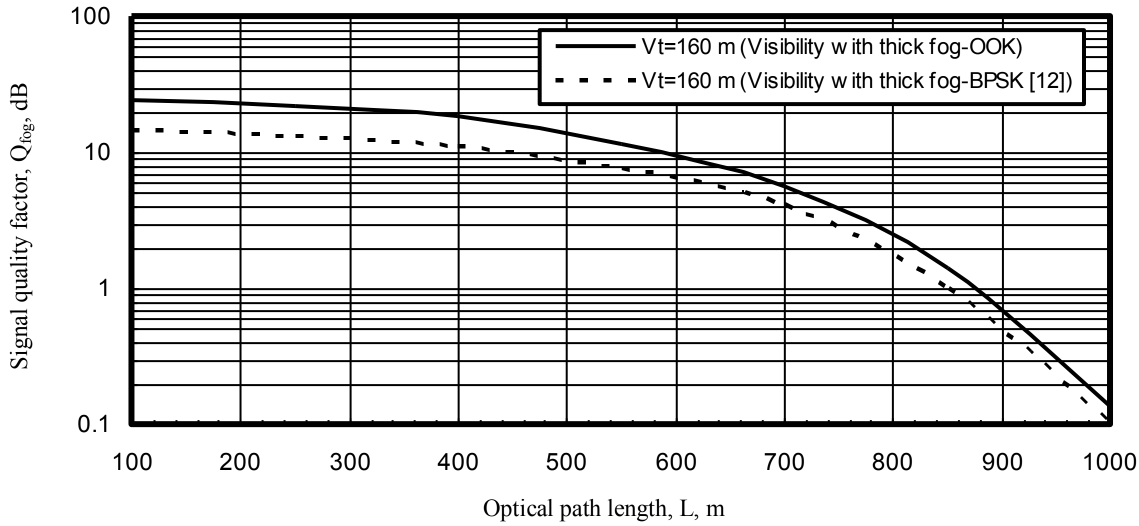

Fig. 25. Signal quality factor in relation to optical path length and visibility with thick fog at the assumed set of the operating parameters.

ISSN: 2278 – 909X

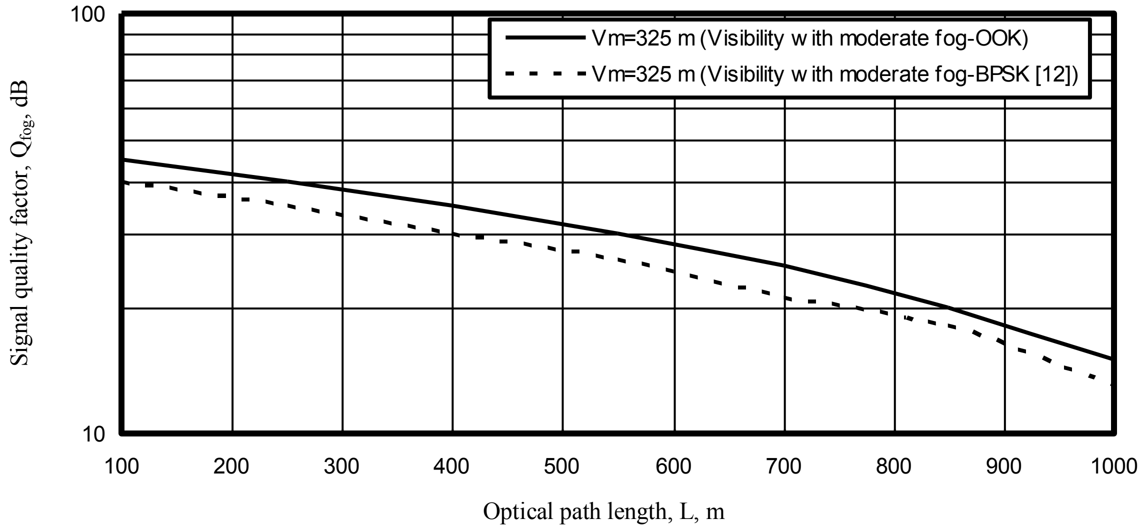

Fig. 26. Signal quality factor in relation to optical path length and visibility with moderate fog at the assumed set of the operating parameters.

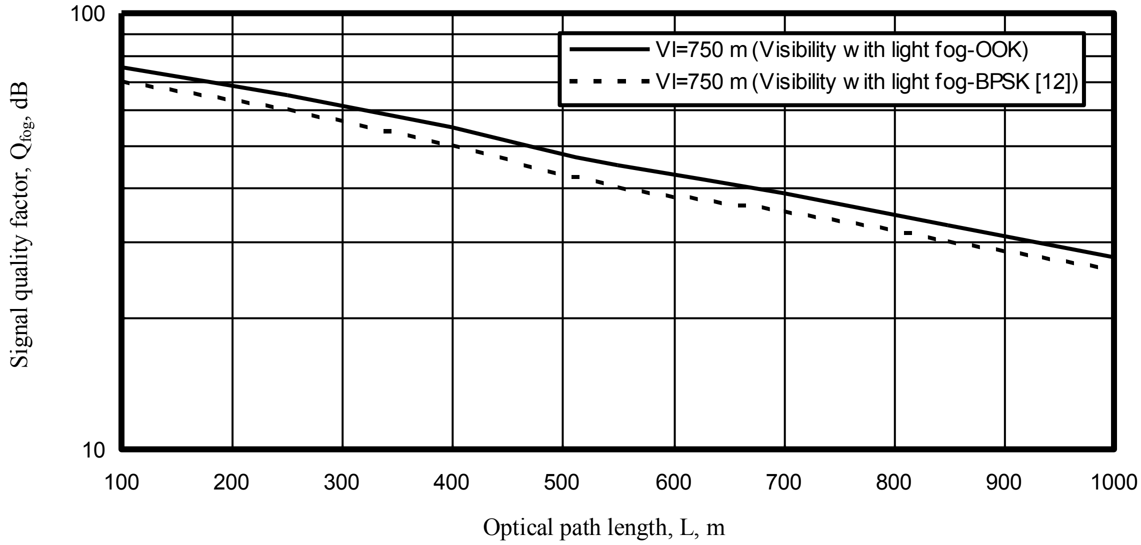

Fig. 27. Signal quality factor in relation to optical path length and visibility with light fog at the assumed set of the operating parameters.

iii) As shown in Figs. (7-10) have demonstrated that as optical path length with different fog density levels increase, this leads to increase in atmospheric signal attenuation. As well as operating optical signal wavelength increases, this results in decreasing of atmospheric signal attenuation for different fog density levels. Moreover it is theoretically found that dense fog level has presented maximum atmospheric signal attenuation in compared with other fog density levels.

iv) Figs. (11-14) have assured that as optical path length with different fog density levels increases, this results in decreasing of signal transmission. As well as operating optical signal wavelength increases, this leads to increase in signal transmission for different fog density levels. It is observed that light fog level has presented maximum signal transmission in compared with other fog density levels.

v) Fig. 15 has indicated that as optical path length with different fog density levels increases, this results in increasing of optical thickness or optical depth of the wireless signal. This simulation result performed at operating optical signal wavelength λ=1550 nm that verified minimum signal scattering and attenuation, thus presented high signal transmission.

vi) Figs. (16-18) have assured that received signal power, transmission data rate and link margin decrease with increasing optical path length for different visibilities at different fog density levels. It is observed that in light fog level has presented maximum received signal power, link margin and transmission data rate in compared with other different fog density levels.

vii) As shown in Figs. (19, 20) have indicated that signal time delay spread increases with increasing optical path length and fog density level. It is theoretically observed that our simulation results with using on-off keying has presented lower signal time delay spread in compared with their simulation

ISSN: 2278 – 909X

results with using binary phase shift keying (BPSK) in Ref. [12].

viii) Figs. (21-23) have assured that background noise power increases with increasing both receiver field of view and optical path length for different fog density levels. It is theoretically found that light fog level has presented the lowest background noise power in compared with other fog density levels.

ix) As shown in Figs. (22-27) have indicated that signal quality factor or signal to noise ratio decreases with increasing both optical path length and different fog density levels. It is theoretically observed that our simulation results with using on-off keying has presented higher signal to noise ratio in compared with their simulation results with using binary phase shift keying (BPSK) in Ref. [12].

V. Conclusions

In a summary, FSO is an option that can be deployed as a reliable solution for high bandwidth short distance enterprise applications. Weather condition is one of the important factors that must be studied in FSO systems. The selection of wavelength is important in order to reduce scattering coefficient and atmospheric attenuation. From the result analysis, FSO wavelength with 1550 nm produces less effect in scattering coefficient and atmospheric attenuation. Short link range between the transmitter and receiver can optimize the FSO system transmission. Based on the analysis, it is recommended to install FSO system with 1550 nm wavelength and optical link range up to 1000 m. As well as we have demonstrated the effect of fog on the FSO link background noise power and signal transmission quality performance by observing transmittance values for a range of received optical power. The FSO system is set to work at the link margin therefore we could investigate the effects of different fog levels. Different fog density levels have presented to observed effects on receiver signal power, link margin, transmission data rate and signal to noise ratio at different transmission distances. Theoretically it is found that the receiver signal power, link margin, data rate and signal transmission quality decreasing with increasing path link but increasing with increasing visibility under fog attenuation conditions. Moreover it is indicated that our simulation results with using on-off keying modulation technique has presented lower signal time delay spread and higher signal to noise ratio in compared with their simulation results with using binary phase shift keying (BPSK) in [12].

References

[1] J. Li, J. Q. Liu, and D. P. Taylor, “Optical communication using subcarrier PSK intensity modulation through atmospheric turbulence channels,” IEEE Trans. Commun., vol. 55, no. 8, pp. 1598–1606, Aug. 2007.

[2] Ahmed Nabih Zaki Rashed, “High Efficiency Wireless Optical Links in High Transmission Speed Wireless Optical Communication Networks,” Accepted for publication in International Journal of Communication Systems, Wiley Publisher, 2013.

[3] M. Uysal, J. Li, M. Yu, “Error Rate Performance Analysis of Coded Free-Space Optical Links over Gamma-Gamma Atmospheric Turbulence Channles,” IEEE Trans. on Wireless Comm., vol. 5, no. 6, pp. 1229 – 1233, 2006.

[4] H. Wu, M. Kavehrad, “Availability Evaluation of Ground-to-Air Hybrid FSO/RF Links,” Int. J. of Wireless Information Networks, vol. 14, no. 1, pp. 33-45, Mar. 2007.

[5] J. M. Kahn, W. J. Krause, and J. B. Carruthers, “Experimental characterization of non directed indoor infrared channels,” IEEE Trans. Commun., vol. 43, pp. 1613–1623, 1995.

[6] C. F. Bohren and D. R. Huffman, Absorption and Scattering of Light by Small Particles, John Wiley and Sons, New York, 1983.

[7] X. Zhu and J. M. Kahn, "Free-space optical communication through atmospheric turbulence channels," IEEE Transactions on Communications, vol. 50, pp. 1293-1300, Aug. 2002.

[8] T. Ohtsuki, "Turbo-coded atmospheric optical communication systems," in IEEE International Conference on Communications (ICC) New York, pp.2938-2942, 2002.

[9] M. Uysal, L. Jing, and Y. Meng, “Error rate performance analysis of coded free-space optical links over gamma-gamma atmospheric turbulence channels,” IEEE Trans. Wireless Commun., vol. 5, no. 6, pp.1229–1233, June 2006.

[10] A. A. Farid, S.Hranilovic, “Outage Capacity Optimization for Free-Space Optical Links With Pointing Errors” journal of lightwave technology, vol. 25, no. 7, july 2007.

[11] W. O. Popoola, Z. Ghassemlooy, and E. Leitgeb, "Free-space optical communication using sub carrier modulation in gamma-gamma atmospheric turbulence," in 9th International Conference on Transparent Optical Networks (ICTON '07) Rome Italy, Vol. 3, pp. 156-160, 2007.

[12] J. Li, J. Q. Liu, and D. P. Taylor, "Optical communication using subcarrier PSK intensity modulation through atmospheric turbulence channels," IEEE Transaction on communications, vol. 55, pp. 1598-1606, 2007.

[13] M. A. Al-Habash, L. C. Andrews, and R. L. Phillips, “Mathematical model for the irradiance probability density function of a laser beam propagating through turbulent media,” Opt. Eng., vol. 40, pp. 1554–1562, 2001.

[14] H. Henniger, O. Wilfert “An Introduction to Free space Optical Communications,” Radio Engineering, Vol. 19, No. 2, June 2010.

[15] J. D. Barry and G. S. Mecherle, “Beam pointing error as a significant parameter for satellite borne, free-space optical communication systems,” Opt. Eng., vol. 24, no. 6, pp. 1049–1054, Nov. 1985.

[16] C. C. Chen and C. S. Gardner, “Impact of random pointing and tracking errors on the design of coherent and incoherent optical intersatellite communication links,” IEEE Trans. Commun., vol. 37, no. 3, pp. 252–260, Mar. 1989.

[17] S. Arnon and N. S. Kopeika, “Laser satellite communication networkvibration effect and possible solutions,” Proc. IEEE, vol. 85, no. 10, pp. 1646–1661, Oct. 1997.

ISSN: 2278 – 909X

[18] Z. Kolkai, V. Biolkova, and D. Biolek, "Model of Atmospheric Optical Channel with Scattering," Latest Trends on Communications, vol. 5, no. 4, pp. 141-144, 2004.

[19] M. S. Awan, L. C. Horwath, S. S. Muhammad, E. Leitgeb, F. Nadeem, M. S. Khan, "Characterization of Fog and Snow Attenuations for Free-Space Optical Propagation," Journal of Communications, Vol. 4, No. 8, pp. 533-445, Sep. 2009.

[20] U. Ketprom, S. Jaruwatanadilok, Y. Kuga, A. Ishimaru, and J. A. Ritcey, "Channel modeling for optical wireless communication through dense fog," Journal of Optical Networking, Vol. 4, No. 6, pp. 291-299, June 2005.

[21] Mazin Ali A. Ali, "Charactriazn of Fog Attenuation for Free Space Optical Communication Link," International Journal of Electronics and Communication Engineering &Technology, Vol. 4, No. 3, pp. 244-255, 2013.

[22] M. Aharonovich and S. Arnon, "Performance improvement of optical wireless communication through fog with a decision feedback equalizer," J. Opt. Soc. Am. A/Vol. 22, No. 8, pp. 1646-1654, Aug. 2005

[23] E. Ferdinandov, and T. Mitsev, "Link Range of Free Space Laser Communication System," Microwave Review Journal, Vol. 9, No. 2, pp. 41-42, Dec. 2003.

[24] J. C. Ricklin, S. M. Hammel, F. D. Eaton, and S. L. Lachinova, "Atmospheric channel effects on free-space laser communication," Journal of Optical and Fiber Communications Research, vol. 3, pp. 111-158, 2006.

Author's Profile

Dr. Ahmed Nabih Zaki Rashed was born in Menouf city, Menoufia State, Egypt country in 23 July, 1976. Received the B.Sc., M.Sc., and Ph.D. scientific degrees in the Electronics and Electrical Communications Engineering Department from Faculty of Electronic Engineering, Menoufia University in 1999, 2005, and 2010 respectively. Currently, his job carrier is a scientific lecturer in Electronics and Electrical Communications Engineering Department, Faculty of Electronic Engineering, Menoufia university, Menouf.

His scientific master science thesis has focused on polymer fibers in optical access communication systems. Moreover his scientific Ph. D. thesis has focused on recent applications in linear or nonlinear passive or active in optical networks. His interesting research mainly focuses on transmission capacity, a data rate product and long transmission distances of passive and active optical communication networks, wireless communication, radio over fiber communication systems, and optical network security and management. He has published many high scientific research papers in high quality and technical international journals in the field of advanced communication systems, optoelectronic devices, and passive optical access communication networks. His areas of interest and experience in optical communication systems, advanced optical communication networks, wireless optical access networks, analog communication systems, optical filters and Sensors. As well as he is editorial board member in high academic scientific International research Journals. Moreover he is a reviewer member in high impact scientific research international journals in the field of electronics, electrical communication systems, optoelectronics, information technology and advanced optical communication systems and networks. His personal electronic mail ID (E-mail:ahmed_733@yahoo.com). His published paper under the title **"High reliability optical interconnections for short range applications in high performance optical communication systems"** in Optics and Laser Technology, Elsevier Publisher has achieved most popular download articles in 2013.

ISSN: 2278 – 909X